

JOURNAL OF SEPARATION SCIENCE

20|2022



www.jss-journal.com

WILEY-VCH

Methods

Chromatography · Electroseparation

Applications

Biomedicine · Foods · Environment

RESEARCH ARTICLE

Comparative analysis of trilobal capillary-channeled polymer fiber columns with superficially porous and monolithic phases toward reversed-phase protein separations

Lacey S. Billotto | R. Kenneth Marcus 

Department of Chemistry, Biosystems
Research Complex, Clemson University,
Clemson, South Carolina, USA

Correspondence R. Kenneth Marcus,
Department of Chemistry, Biosystems
Research Complex, Clemson University,
Clemson, SC 29634, USA.
Email: marcusr@clemson.edu

A trilobal capillary-channeled polymer fiber stationary phase is evaluated for its performance for intact protein separations under reversed-phase high-performance liquid chromatography conditions. The separation quality, operational characteristics, and protein dynamic loading capacity on the fiber phases are compared to commercially-available superficially porous and monolithic columns. The trilobal or “y-shaped” polypropylene fiber phase was employed to separate a synthetic mixture of five proteins (having diverse chemistries and molecular weights). The separation quality was evaluated based on the resolution, peak heights/recoveries, peak widths, and peak areas. The present work illustrates the unique ability to operate at higher linear velocities (47.5 mm/s) while maintaining lower back pressures (~4 MPa), faster separation times (<8 min), and faster gradient rates using the fiber columns while yielding comparable chromatographic performance to the commercial columns. The separations employing the commercial stationary phases operate at lower linear velocities (~3.0 mm/s), higher back pressures (~9 MPa), require longer separation times (10 min), and require slightly higher compositions of organic mobile phase to effect protein elution. Likewise, based on breakthrough loading analysis of lysozyme and bovine serum albumin, the trilobal, polypropylene C-CP fiber column stationary phases demonstrate 3–9X greater binding capacities on a bed volume basis versus the commercial columns.

KEYWORDS

capillary-channeled polymer fibers, monolith, proteins, reversed-phase, superficially porous

Article Related Abbreviations: α -chym A, alpha-chymotrypsinogen A; C-CP, capillary-channeled polymer; DI-H₂O, de-ionized water; lyso, lysozyme; PP, polypropylene; PPY, trilobal, polypropylene C-CP fiber; trans, transferrin.

1 | INTRODUCTION

RP-LC is one of the most widely used separation modalities for complex mixtures of small molecules. RP chromatography methods owe their versatility to the ability of the stationary phases to isolate target analytes based on their relative polarity/hydrophobicity [1, 2]. Particularly in

biochemistry-related fields, RP-LC has proven to be useful for the isolation of small molecules, including peptides, drugs, and metabolites, but has been extended to include proteins and other macromolecules [3–7]. The utility of RP-LC toward large molecules is augmented by convenient gradient separations to resolve chemically similar (albeit complex) molecules [2, 4].

Porous silica support phases modified with organic ligands are by far the most commonly applied in RP-LC applications [1, 2], extending to the separation of biomacromolecules such as peptides and proteins [4, 8–10]. In the case of biomacromolecules, the chromatographic characteristics and figures of merit are affected by the analytes' affinity for the hydrophobic stationary phases (and perhaps the support) [4], yielding a complex set of potential interactions. As another variable, the addition of modifiers is beneficial in preventing secondary equilibrium effects based on the ionization of amine or carboxylic acid groups in proteins, etc. Most common is the addition of acids, such as TFA [4, 11, 12], where the low pH is favorable due to the increased solubility of proteins and a greater extent of ionization of solvent-accessible amine groups. Unfortunately, the use of even low percentages of TFA in the RP solvent systems can be harmful to the stability of silica-based stationary phases [13]. To this end, the use of polymer-based stationary phases eliminates this issue. In addition, polymeric supports can be prepared in a large variety of shapes and chemistries [14–18].

A fundamental challenge in the LC separation of biomacromolecules, regardless of the modality, deals with their transport dynamics in the mobile and support phases [1, 19, 20]. Proteins have inherently poor diffusional/mass transfer characteristics in the bulk mobile phase and within the porous supports, colloquially referred to as van Deemter C-term effects, leading to excessive band broadening. Another potential challenge in using fully-porous supports is the potential for exclusion from the pore volumes, limiting binding capacities, and introducing size-exclusion aspects to the separations. Silica-based superficially porous and monolithic supports were developed to address the mass transfer limitations in the solid phase, which hinders separations, particularly toward achieving higher protein throughput [21–27]. The typical 2.7 μm diameter fused-core particles boast better loading characteristics, higher peak capacities, shorter diffusion paths, and improved separation speeds for biomolecules than totally porous particles of the same size. [24, 27–32]. Towards the same end, monolithic columns are composed of a single continuous rod-like structure that produces a highly permeable column, with mass transport through the mesoporous structure enhanced by convective processes [25, 33–35]. Monolith columns have received attention for biomacromolecule separations [36–38], promoting

faster separations of proteins than packed-bed columns [39]. Despite the benefits of both stationary phase types relative to biomacromolecule separations, neither is without disadvantages. The flow between the small particles can impose strong shear forces leading to conformational changes, bond breakage, and thus, altered structures of the analyte [27], an issue when further protein characterization is desired. Additionally, the small-particle columns are prone to fouling in the presence of complex bio-media [27]. In the case of monolithic columns, physical inhomogeneity can yield higher asymmetry factors, lower resolution, and larger dead volumes [26, 39].

These limitations, coupled with the potential for the degeneration of silica-based supports, have opened the path for polymer-based stationary phases to be used in RP protein separations. The rigid, porous structures of polymeric beads are virtually unaffected by the environment, with interconnected cavities allowing for the diffusion of molecules [34]. Polymer-based stationary phases, including monoliths, have chemical advantages over silica materials, including a wide range of pH stability and a wide diversity of base material and surface chemistries [13, 14, 18, 34, 40–42].

Beyond potential chemical advantages, movement to polymeric materials provides the potential for different physical formats. Among these are natural and synthetic fibers as reviewed by Marcus [18, 42]. A vast number of chemistries and shapes have been described, with the primary practical constants being very low material costs and solute transport assisted by convective diffusion (i.e., the coupling of diffusional and advective mass transport) [41, 43–47]. While the surface areas of most fiber materials pale in comparison to porous media, relatively low back pressures are coupled with enhanced mass transport; near-ideal traits for macromolecule separations. This laboratory has developed capillary-channeled polymer (C-CP) fiber columns, employed as combined support/stationary phases for protein separations [48, 49]. The C-CP fibers are created via melt extrusion from commodity polymers including polypropylene (PP), polyester, and nylon-6, providing a range of hydrophobicities and ionic character toward RP [48, 50], IEC [51, 52], and hydrophobic interaction chromatography [52, 53] protein separations. Likewise, a rich set of simple surface modification chemistries provides more efficient ionic separations [54, 55] and generates selective affinity phases [56–58].

Hydrodynamic benefits of the C-CP fiber column arise from the thousands of parallel, 1–4 μm diameter channels that are formed in the co-linear packing of the $\sim 50 \mu\text{m}$ wide, eight-channeled fibers [59, 60] and the practically non-porous matrices [61]. Commonly, the van Deemter equation (Equation (1)) describes column efficiency and performance in isocratic separations, allowing a better

understanding of underlying limitations.

$$H = A + \frac{B}{u} + C * u \quad (1)$$

A number of detailed studies using C-CP fiber phase separations of proteins point to the van Deemter A-term being the primary limiting aspect, with C-term broadening being virtually non-existent at linear velocities of up to 100 mm/s [60, 62, 63]. The lack of C-term broadening is a direct result of the non-porous nature of the fiber surfaces with respect to the size of proteins as well as enhanced mobile phase mass transfer at relatively high linear velocities [60, 61, 64]. As the A-term reflects the variance in the solute paths, it represents the uniformity (or lack thereof) of the support phase packing. The original C-CP fibers entailed an eight-channeled structure, each having a different diameter. As such, the uniformity of the packing suffered, yielding plate heights of single millimeters for protein solutes [60].

The recent introduction of a trilobal (y-shaped) PP C-CP fiber phase was projected to yield much better uniformity among the inter-fiber channels [63]. As revealed through SEM imaging, the Y-shaped fibers yield improved packing densities and increased channel uniformity versus the eight-channel version [63]. Following an investigation of the roles of fiber packing density (i.e., interstitial fraction), plate heights were reduced from ~1.5 to ~0.2 mm for BSA at a linear velocity of 25 mm/s. The effort also included optimization of the mobile phase flow rate (i.e., linear velocity) and RP gradient rate on the resolution of key pairs in a synthetic mixture of six proteins. Ultimately, the trilobal fibers provided better separation quality. The platform also performed very well in the high throughput, LC-MS analysis of intact proteins [65].

Herein, a systematic comparison is made between the PP C-CP fibers having a y-shaped perimeter (termed PPY fibers) and commercially-available superficially porous and monolithic columns, sold explicitly for RP protein separations. The studies presented here complement those of a recent report from this laboratory, wherein the PPY format was benchmarked versus a different RP superficially porous column and an SEC platform in terms of performance across biomolecules ranging up to a molecular weight of 660 kDa [66]. Efficient fiber column separations spanned the entirety of the protein suites, whereas the other two formats were limited to the low and high ends of the mass scale, respectively. Here, attention is paid to physico-chemical comparisons of the respective phases' characteristics. Points of comparison include analyte elution order, operating system back pressure, dynamic binding capacities determined by frontal (breakthrough) analysis, and chromatographic figures of merit. The commercial columns were operated under conditions recommended

by their manufacturers. The much-improved chromatographic performance realized with the trilobal shape, in combination with lower back pressures, higher bed volume binding capacities, and low materials cost bode well for future analytical-scale RP protein separations.

2 | MATERIALS AND METHODS

2.1 | Chemicals and sample preparation

HPLC-grade ACN (Millipore, Merck, Germany), deionized water (DI-H₂O) (milli-Q water; 18.2 MΩ-cm, Millipore, Merck, Germany), and TFA (Sigma-Aldrich, St. Louis, MO, USA) were used for sample and mobile phase preparation. Mobile phase A consisted of DI-H₂O with 0.1% TFA, and Mobile phase B was made up of ACN and 0.1% TFA. Ribonuclease A (13.7 kDa), cytochrome c (12.0 kDa), lysozyme (lyso) (14.3 kDa), transferrin (trans) (80 kDa), uracil, BSA (66.5 kDa), and alpha-chymotrypsinogen A (α-chym A) (25 kDa) were each purchased from Sigma-Aldrich. These proteins represent a range of hydrophobicities and molecular weights, ranging from approximately 12–80 kDa. Stock solutions (2 mg/ml) of each protein were prepared in PBS (1x), purchased from Hyclone Laboratories (Logan, Utah, USA), and diluted with DI-H₂O and 0.1% TFA to the working concentration, ~0.02 mg/ml, on the day of the analysis.

2.2 | Chromatographic columns

The trilobal, PPY C-CP fibers used in the current work were melt-extruded by the Department of Material Science and Engineering at Clemson University using spinnerets that yield a 35-fiber bundle. SEM imaging of the PPY fiber-packed columns reveals fiber leg lengths of ~20 μm and total perimeters of 120 μm, with column uniformity appearing superior to the original eight-channeled fibers [63]. Columns here were prepared by packing the PPY fibers using previously described methods [26, 39, 48]. The shell of the column, through which the fibers were pulled, was polyether ether ketone tubing purchased from Cole-Parmer (Vernon Hills, IL). The column length was approximately 300 mm with an inner diameter of 0.762 mm. Based on preliminary studies, 630 total fibers of PPY were packed into each C-CP column. Before all chromatographic trials, the C-CP fiber columns were washed at flow rates varying from 0.1–1.0 ml/min with ACN, then DI-H₂O until a stable absorbance baseline was obtained at 216 nm. Varying the flow rate is important to ensure a stable baseline can be achieved across the flow rates utilized in the experiments. Washing is essential to remove

any anti-static coatings applied to the fiber following the extrusion process [49, 63].

To better understand and benchmark the PPY fiber column performance in RP-LC protein separations, two commercial columns designed specifically for RP protein separations were evaluated. The first column was the Agilent Infinity Lab Poroshell 120 column (Agilent Technologies, Santa Clara, CA). The column dimensions were 3.0×50 mm and packed with superficially porous, $2.7 \mu\text{m}$ diameter silica particles with a 12 nm average pore size and an EC-C18 bonded phase applied to the porous outer layer. The second column was the Chromolith® Performance RP-8e column (Merck KGaA, Darmstadt, Germany). The monolithic column dimensions were 4.6×100 mm, having $2 \mu\text{m}$ macropores and 13 nm mesopores within the single high-purity, highly porous, silica gel-derived rod with C-8 ligation. In all cases, the commercial columns were operated as per the manufacturer's instructions for protein separations.

Uracil and lyso (5 μl injections of 20 $\mu\text{g}/\text{ml}$, each) were used as the two hydrodynamic probe species for the van Deemter characterization data under conditions where each solute was not chemically retained in the phases [51]. (This volume/concentration combination is below the onset of overload conditions for the low-volume fiber columns [67].) The use of these two markers provides complementary information as uracil can fully access the pore structures of each phase, while lyso reflects those surfaces where the target proteins have access. On the PPY column, uracil was eluted with isocratic mobile phase conditions of 5% mobile phase B and 95% mobile phase A, while lyso was eluted in isocratic mobile phase conditions consisting of 60% mobile phase B and 40% mobile phase A. For the superficially porous and monolithic columns, uracil and lyso were eluted with the same isocratic conditions of 60% mobile phase B and 40% mobile phase A.

Marcus and Nelson described an approach to optimize rapid protein separations on C-CP fiber columns through manipulation of the gradient steepness and mobile phase flow rate [49]. Here, a similar starting gradient was employed with mobile phases A and B, at a flow rate of 0.5 ml/min in 15 min (6.67% change per minute). This gradient was used to determine the solvent strength needed to elute each protein in the suite. The use of 0.1% TFA in the mobile phase is important in the elution characteristics in RP chromatography, lowering the pH to ~ 2 , and effectively protonating the carboxylic acid groups of the proteins [8]. This causes an increase in the hydrophobicity and retentivity of the proteins [8], while also minimizing their overall charge variability. It is important to reiterate that, different from the case of derivatized silica phases, the PPY stationary phase surface chemistry is not affected by changes in solvent pH.

2.3 | Instrumentation and methods

Chromatographic experiments were performed on two Dionex Ultimate 3000 HPLC systems (LPG-3400SD quaternary pump, WPS-3000TSL autosampler, and either a VWD-3400RS or MWD-3000 UV-Vis detector; ThermoFisher Scientific, Sunnyvale, CA) operating under the control of Chromeleon 6.8 and 7 data systems, respectively. To provide better reproducibility and lower plate heights, the auto-injection mode on the WPS-3000TSL autosampler-equipped with the VWD-3400RS detector was used to obtain the fundamental van Deemter-related data, employing 5 μl injections and 5°C temperature control. 20 μl injections of a five-protein mixture were run in the manual injection mode on the LPG-3400SD quaternary pump with the MWD-3000 UV-Vis detector due to higher protein sensitivities realized in that system. The sensitivity difference is due to the increase in flow cell path lengths between the instruments. All solvent gradients, flow rates, and loading amounts were optimized using the manual injection mode. All data points were collected in triplicate ($n = 3$) for each experiment unless otherwise stated. Solvent baseline absorbance values from blank injections were subtracted from each protein separation. It must be stated that for the quality metrics provided herein (peak widths, resolution, etc.), the inputs were taken from the chromatographic data and calculated within the instrument data system.

3 | RESULTS AND DISCUSSION

3.1 | Hydrodynamic characterization

The hydrodynamic efficiency of an HPLC column is generally evaluated in terms of van Deemter plots (plate height (H) as a function of linear velocity (U_0)). The linear flow velocity (Equation (2)) was calculated for each column format using the determined interstitial fractions (Equation (3));

$$U_0 = \frac{F}{r^2 * \pi * \epsilon_i} \quad (2)$$

where r is the internal radius of the column. The interstitial fraction (ϵ_i) was determined experimentally using the retention time of unretained uracil injections as described in Equation (3);

$$\epsilon_i = \frac{F (t_r - t_0)}{V_c} \quad (3)$$

where F is the mobile phase volumetric flow rate, t_r is the on-column retention time, t_0 is the elution time for

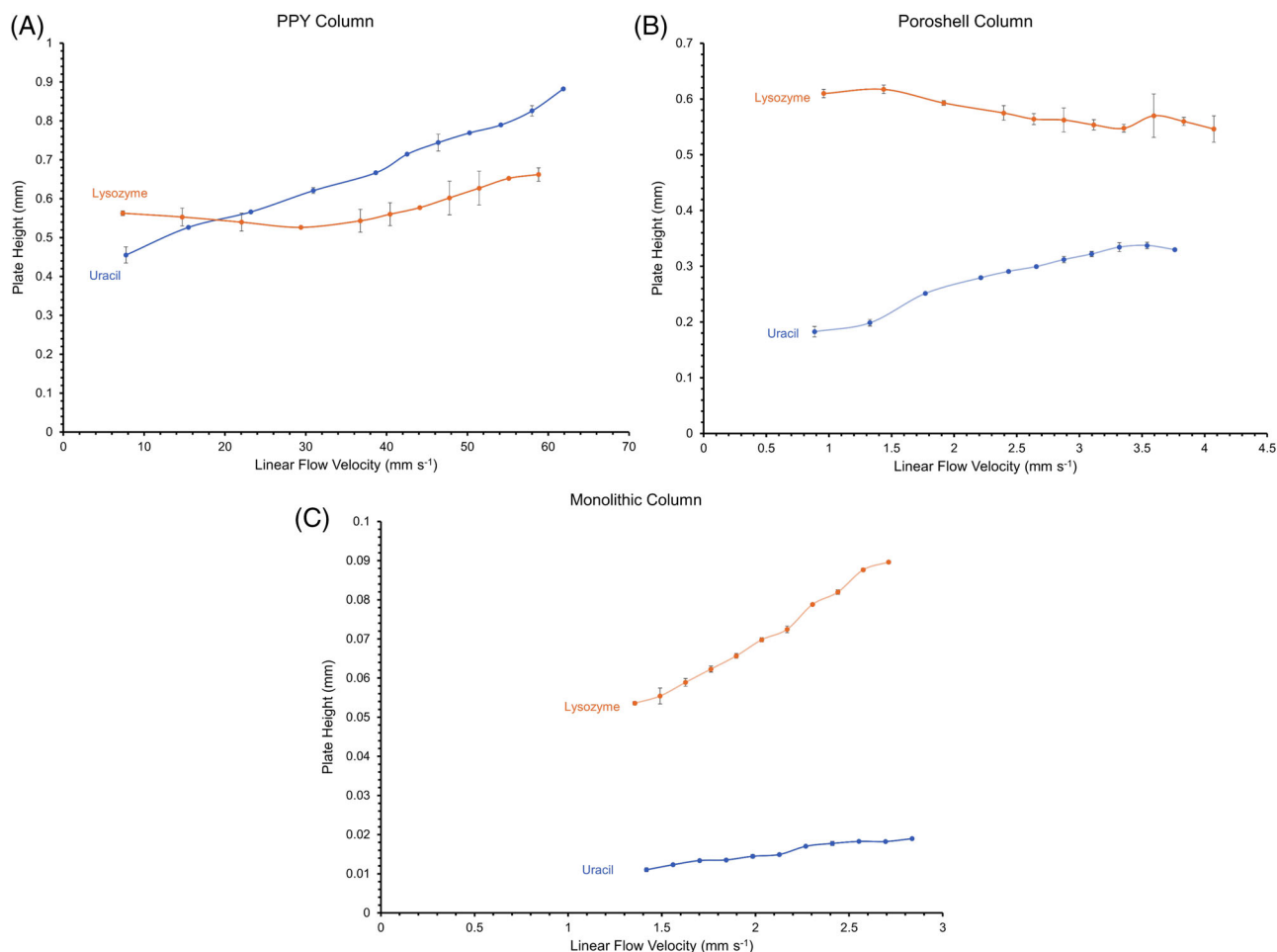


FIGURE 1 van Deemter plots for (A) the trilobal, polypropylene C-CP fiber (PPY C-CP) fiber column, (B) superficially porous, and (C) monolithic commercial columns. The uracil and BSA conditions on the PPY column were divided by 10 to present all values on the same scale

the uracil without a column present, and V_c is the volume of the empty column. The ε_i was found to be 0.473 for the PPY fiber column, comparable to the previously determined value of 0.457 for the same format [63]. This lower interstitial fraction compared to the eight-channeled fibers ($\varepsilon_i = 0.616$) [63] suggests more restricted flow but with greater exposed fiber surface area (i.e., more fibers) to affect separations. Additionally, the low interstitial fraction reflects shorter diffusional distances between opposing fiber surfaces. Finally, the lower interstitial fraction results in higher linear velocities at the same volume flow rates, which should improve solute mass transfer characteristics according to the Leveque equation [64, 68]. The determined ε_i values for the commercial columns were: superficially porous = 0.532, and monolithic = 0.707. While the interstitial fraction reflects the free volume, opposite of the available surface area for adsorption, it also bears on the hydrodynamic throughput, as lower interstitial fractions yield higher mobile phase linear velocities for the same volume flow rates, a first approximation at reducing on-column residence time and B-term broadening [69].

The van Deemter plots, for experiments performed in triplicate, are shown in Figure 1. The PPY capillary column (Figure 1A) was able to operate at much higher linear velocities (~13X and 16X) than those of the superficially porous (Figure 1B) and the monolithic (Figure 1C) columns, respectively, while still obtaining comparable van Deemter terms. For the respective columns, the volume flow rates ranged from 0.1–0.8 ml/min for the fiber column, 0.1–0.8 ml/min for the superficially porous, and 1–2 ml/min for the monolith. The back pressures realized at the maximum flow rates were ~5, 12, and 10 MPa, respectively. Qualitatively, the resulting plots for the three column types are quite different, though, within each solute/column set, the precision in the values for each test condition is quite good. Across both probe species and the operable flow velocities, the monolithic column was able to consistently achieve lower plate heights (0.01–0.1 mm), with the fiber and superficially porous columns yielding approximately the same order of magnitude, on the 0.2–0.6 mm level. The most glaring difference among the van Deemter plots is the fact that particularly at the

TABLE 1 The absolute value of the van Deemter parameters for the three columns using uracil and BSA as solutes

Column	Sample	A Term (mm)	B Term (mm ² /s)	C Term (s)	R ²
PPY	Uracil	0.378	0.179	7.7E-03	0.993
	Lyso	0.663	0.661	2.6E-03	0.993
Superficially porous	Uracil	0.232	0.079	0.036	0.968
	Lyso	0.603	0.028	5.4E-03	0.823
Monolithic	Uracil	0.011	8.9E-03	3.8E-03	0.972
	Lyso	0.027	0.039	0.038	0.996

very much higher (>25X) linear velocities of the C-CP fiber column, the determined plate heights for the protein (lyso) are lower than the small molecule (uracil). In this case, as observed in earlier works, the uracil molecule has some limited access to the pore structure of the fibers [60, 61], while the protein is completely excluded. On the contrary, the two silica-based supports show appreciable differences between the two probe molecules, with the protein yielding appreciably higher plate heights. In general, the increase in plate height for the protein is more immune to increases in linear velocity in the case of the superficially porous material versus the monolith.

The extracted van Deemter constants for the three column types are presented in Table 1. Going through the respective terms sequentially allows for deeper levels of comparison, beyond the qualitative aspects depicted in the plots of Figure 1. In the case of the van Deemter A-term, which reflects the variability in the flow paths within the column beds, the uniformity of the solute transport profiles is seen to be much better for the monolithic column than either the fiber or the packed bed formats. This difference is not particularly surprising as the majority of that column's bed volume is open space through the pore structure. The fact that the A-term is the largest contributor to broadening in the case of the fiber materials has long been realized [60, 62], though the values here and in previous work with the trilobal shape [63] are much smaller than the original 8-channeled fiber structure. Certainly, there is still room for improvement in the packing quality. The van Deemter B-term reflects the extent of longitudinal (diffusive) broadening that naturally occurs. In the case of the two commercial columns, the B-terms are relatively small contributors to overall broadening, but the fact that the values for the fiber column are multiple times larger is somewhat of a surprise. Initially, one might expect that the column format having the highest linear velocity would experience the lowest extent of this form of broadening. What is seen here though, and in previous efforts [60], is a reflection of the lack of tortuosity in the basically open, parallel channels in the fiber bed. The lower pressure drop of the fiber column may also play a role in allowing higher solute diffusivity versus the commercial columns.

Of course, the greatest challenge in the LC separation of biomacromolecules revolves around processes related to the van Deemter C-term. Each of the tested phases has been developed explicitly to address these issues. As seen in Table 1, this aspect is where the fiber phase shows its most demonstrative advantages. As could be gleaned from the responses in Figure 1A, both of the test solutes display little C-term character, with the term being quantitatively smaller for the protein versus uracil. Interestingly, the values are not so distinct, or as might be expected, for the commercial phases. Specifically, the C-term for uracil is smaller than for lyso in the case of the monolithic column. In general, the determined van Deemter constants provide some insight into the on-column broadening mechanisms and certainly combine to bear out the overall lower plate heights seen for the monolith.

3.2 | Optimization of RP separations on trilobal PP fiber phases

To be sure, the RP gradient elution of proteins is a complex process. Different from small molecule separations, the predominately hydrophobicity-driven adsorption of the macromolecules to the stationary phase involves multiple points of contact, having different levels of affinity for the phase. As such, the degree of phase surface ionization, the ionization of the protein functional groups, the extent of unfolding, and many other factors affect how a single protein interacts with a phase. Depending on the actual stationary phase in question, solvent linear velocity can also be a factor. Ultimately, proteins do not generally spontaneously release from a surface at a given mobile phase composition, but rather elute across a band of solvent strengths [5, 6, 9]. Multiple previous studies have laid the experimental approaches to RP gradient optimization relative to RP protein separations on C-CP fiber phases [48, 50, 63]. In order to determine the gradient percentage change that yielded the most favorable separation conditions (though still comparable to the other columns) based on resolution and peak widths, three solvent gradient breadths ranging from 15% to 50% B, 20% to 50% B, and

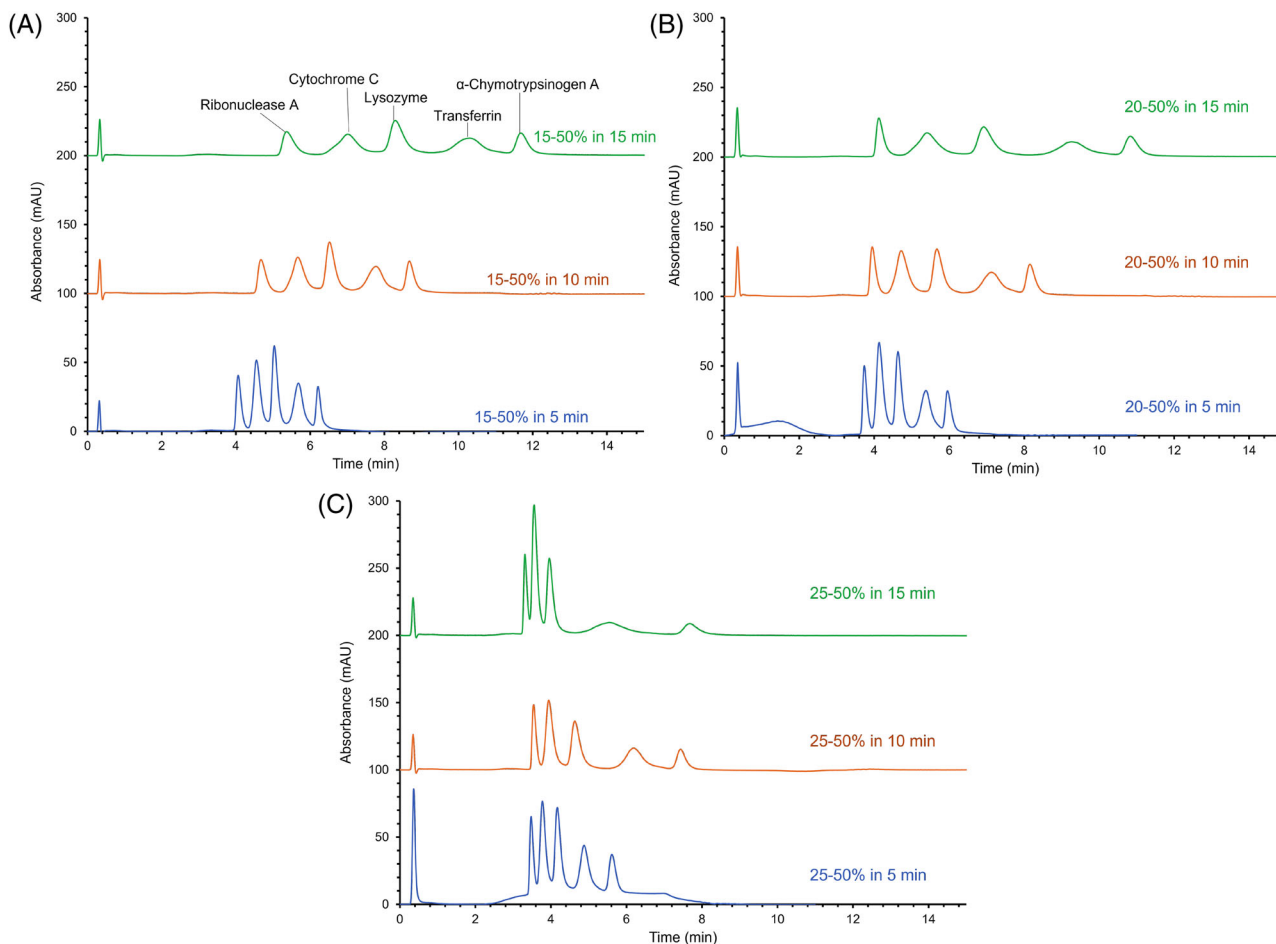


FIGURE 2 Comparison of chromatograms as a function of gradient rate for the polypropylene (PPY) column in 5, 10, and 15 min. (A) Gradient of 15%–50% B (ACN and 0.1% TFA). (B) Gradient of 20%–50% B (ACN and 0.1% TFA). (C) Gradient of 25%–50% B (ACN and 0.1%)

25% to 50% B, were performed across run times of 5, 10, and 15 min, each at a flow rate of 0.5 ml/min. Representative chromatograms for each experimental condition are presented in Figure 2, while the quantitative metrics of the peak width (full width at half-maximum) for the first and last eluting peaks and the determined resolution for each of the critical pairs are presented in Table 2.

Each of the chromatograms has the same general character in terms of the protein elution order (as they should): ribonuclease A, cytochrome c, lyso, trans, and α -chym A. In each case, test mixtures were injected in a solvent of 100% A, with the gradient program initiated 1 min following the injection. Across the set of conditions, the breadth of the solvent window affects both the nominal retention times and peak spacing, with the rate of change within that window having a larger effect on the peak widths. As the critical elution percentage for the first protein (Ribo) is close to 30% B, the shorter gradient windows provide earlier elution times, while the use of more shallow gradients (longer gradient times) provides more temporal displacement between the eluting species. As would be expected,

it is easily seen that the shortest gradient times (highest change rates) provide for the more narrow peaks, with the coincident increases in absorbance peak heights.

A closer inspection of the quantitative figures of merit in Table 2 illustrates the profound effect that faster gradient rates have on minimizing the peak widths for the latter-eluting solutes, typically reducing the $W_{1/2}$ values by a factor of 2 in decreasing the gradient time from 15 to 5 min. Importantly, there are no deleterious effects seen in terms of peak asymmetry in the use of the highest gradient rates. The overall impact of faster gradients regarding the determined resolution characteristics is minimal. While the peaks become more narrow, the time between the peaks changes fairly proportionally, and so the basic benefit is simply improving analytical throughput without real sacrifice in separation quality, which is not necessarily common in the realm of protein chromatography. One negative aspect of the use of the faster gradient times is the lack of complete baseline resolution, and indeed some non-ideal responses appear in the chromatographic background. Therefore, based on the ability to achieve true

TABLE 2 Peak widths (first and last eluting protein) and critical pair resolution values for the varying gradient rates and times on the polypropylene (PPY) column. Protein name in parenthesis, first of each pair

Gradient rate (%)	Time (min)	$W_{1/2}$ First	$W_{1/2}$ Last	R_1 (Ribo A)	R_2 (Cyto c)	R_3 (Lyso)	R_4 (Trans)
15–50	5	0.149	0.146	1.61	1.47	1.66	1.43
	10	0.235	0.236	1.97	1.60	1.97	1.47
	15	0.341	0.330	2.20	1.63	2.11	1.51
20–50	5	0.128	0.184	1.43	1.56	1.76	1.36
	10	0.168	0.262	1.77	1.78	2.03	1.48
	15	0.209	0.364	1.92	1.75	2.34	1.65
25–50	5	0.109	0.213	1.27	1.43	1.88	1.71
	10	0.120	0.263	1.40	1.72	2.32	1.81
	15	0.100	0.431	1.13	1.46	1.72	1.84

$$R = 2(t_2 - t_1)/w_1 + w_2.$$

baseline resolution, reduced broadening as indicated by peak widths, and the decreased use of the organic mobile phase necessary to produce similar results, the gradient window of 25–50% B over a 10-min gradient interval was chosen for the current work.

Previous parametric optimization of the eight-legged C-CP fibers pointed to three primary effects of increasing solvent flow rates, that is, linear velocity. The first is a narrowing of peak widths as the post-desorption transit from the column is faster [49, 50]. The second effect is a lowering of the percentage of solvent B required to affect elution, hypothesized as a lowering of the amount of protein surface contact under increased shear conditions. The final effect is a lower absorbance measurement recovery as the proteins elute in greater solvent volumes per unit time, that is, greater dilution. Having defined the fact that only a 25–50% B gradient range was required for the protein suite, the different gradient rates (5, 10, and 15 min) were evaluated across flow rates ranging from 0.5 to 0.8 ml/min (43–69 mm/s), increasing by 0.1 ml/min increments. Chromatograms representing each of the varying flow rates at different gradient time intervals can be seen in Figure 3. In these chromatograms, it was observed that as the flow rate increased in concert with longer gradient times, the absorbance responses are both diluted and broadened (most dramatically for trans), resulting in a reduction or complete loss of resolution as presented in Table 3. Indeed, as seen in the Table, the performance was degraded so severely as to be useless. For all of the gradient times, the peak elution times would decrease by approximately 1 min, moving from the 0.5 to 0.8 ml/min flow rates, regardless of the solute. This consistency implies that the post-desorption improvement in transport was universal. What was not so pronounced as in previous efforts was that the actual solvent strength for elution was not affected by higher linear velocities. Ultimately, it was observed that the solute peak widths were more driven by the gradient rate,

than the mobile phase linear velocity. Based again on the ability to achieve clear baseline resolution across the five-protein suite, and nominally good overall throughput and absorbance responsivity, the optimal flow rate for the five-protein suite, at a gradient time of 10 min, was determined to be 0.6 ml/min.

3.3 | Comparison of separation quality across column types

Having determined a generalized RP gradient method for the separation of the five-protein test mixture, comparisons with the commercial ‘protein’ columns are in order. Surely, the first level of assessment involves the basic separation quality in terms of the elution characteristics. So as not to bias the results, the superficially porous and monolithic columns were run at their manufacturer-suggested conditions of 0–60% B in 10 min and at flow rates of 0.8 and 2 ml/min, respectively. The optimized conditions for each of the three columns are presented in Table 4. In each case, the protein mixture content, injection conditions, and general procedural steps were held constant.

The protein separations presented in Figure 4 are plotted on the same absorbance and time axes for the sake of ready visual comparison. In addition, the RP gradient programs are incorporated into the chromatograms. It is important to note that the commercial columns involve steeper gradients, beginning at a 0% B composition, while the fiber column begins its gradient at 25% B. The much higher gradient rate for those columns is immediately evident in yielding more narrow elution bands (and thus higher peak absorbances) for the protein solutes. Also seen, the proteins elute at shorter times in the case of the fiber column, simply by the offset of the gradient start point. Finally, it is seen that not all of the proteins are recovered from the monolithic column, as the trans shows a very minor peak

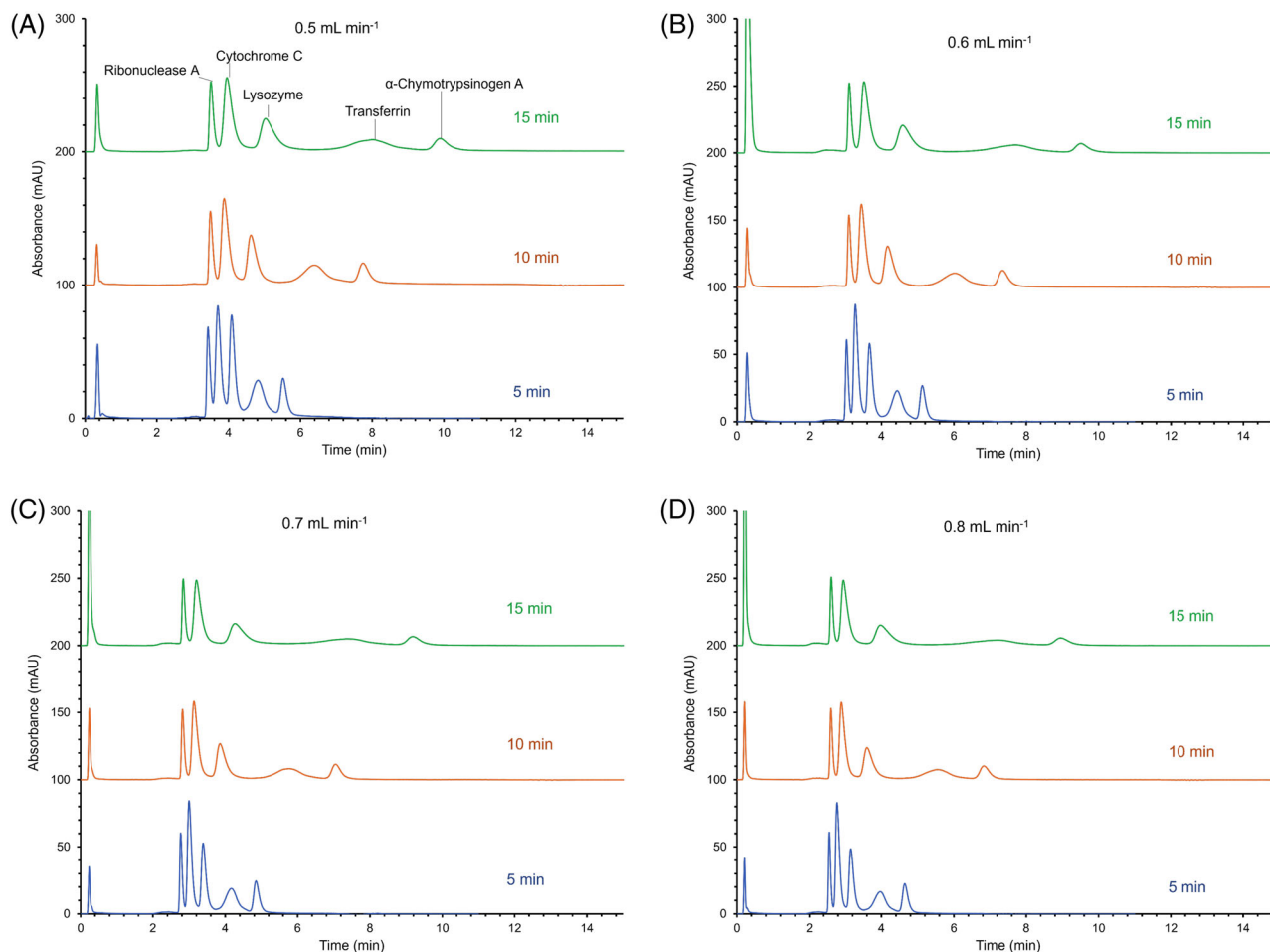


FIGURE 3 Comparison of chromatograms as a function of flow rate for the polypropylene (PPY) column at a gradient of 25–50% B (ACN containing 0.1% TFA) at 5, 10, and 15-min gradients. The flow rates vary from (A) 0.5 ml/min, (B) 0.6 ml/min, (C) 0.7 ml/min, and (D) 0.8 ml/min

TABLE 3 Peak widths (first and last eluting protein) and critical pair resolutions for the varying flow rates and gradient times on the polypropylene (PPY) column

Flow rate (ml/min)	Time (min)	$W_{1/2}$ First	$W_{1/2}$ Last	R_1 (Ribo A)	R_2 (Cyto c)	R_3 (Lyso)	R_4 (Trans)
0.5	5	0.103	0.212	1.23	1.44	1.67	1.52
	10	0.116	0.314	1.35	1.76	2.14	1.61
	15	0.125	0.429	1.38	1.84	2.23	N/A
0.6	5	0.087	0.175	1.26	1.58	1.81	1.56
	10	0.097	0.291	1.40	1.84	2.24	1.57
	15	0.106	0.382	1.41	1.96	7.30	N/A
0.7	5	0.076	0.170	1.33	1.67	1.79	1.49
	10	0.085	0.279	1.42	1.92	2.16	1.44
	15	0.090	0.387	1.44	1.98	7.20	N/A
0.8	5	0.068	0.167	1.33	1.70	5.70	1.56
	10	0.076	0.290	1.39	1.90	6.75	N/A
	15	0.082	0.410	1.41	1.90	6.95	N/A

$$R = 2(t_2 - t_1)/w_1 + w_2.$$

N/A – not distinguishable to calculate resolution.

TABLE 4 Optimized chromatographic conditions for RP-HPLC of a five-protein mixture on a polypropylene (PPY) C-CP fiber column, along with conditions recommended for commercial superficially porous, and monolithic columns

	C-CP (PPY)	Superficially porous	Monolithic
Mobile Phase A	0.1% TFA in DI-H ₂ O	0.1% TFA in DI-H ₂ O	0.1% TFA in DI-H ₂ O
Mobile Phase B	0.1% TFA in ACN	0.1% TFA in ACN	0.1% TFA in ACN
Flow Rate	0.6 ml/min	0.8 ml/min	2.0 ml/min
Linear Flow Velocity	46.4 mm/s	3.54 mm/s	2.83 mm/s
UV Absorbance	216 nm	216 nm	216 nm
Gradient Rate	25-50% B over 10 min	0-60% B over 10 min	0-60% B over 10 min
Percent Change per Unit Time	2.5% B/min	6.0% B/min	6.0% B/min

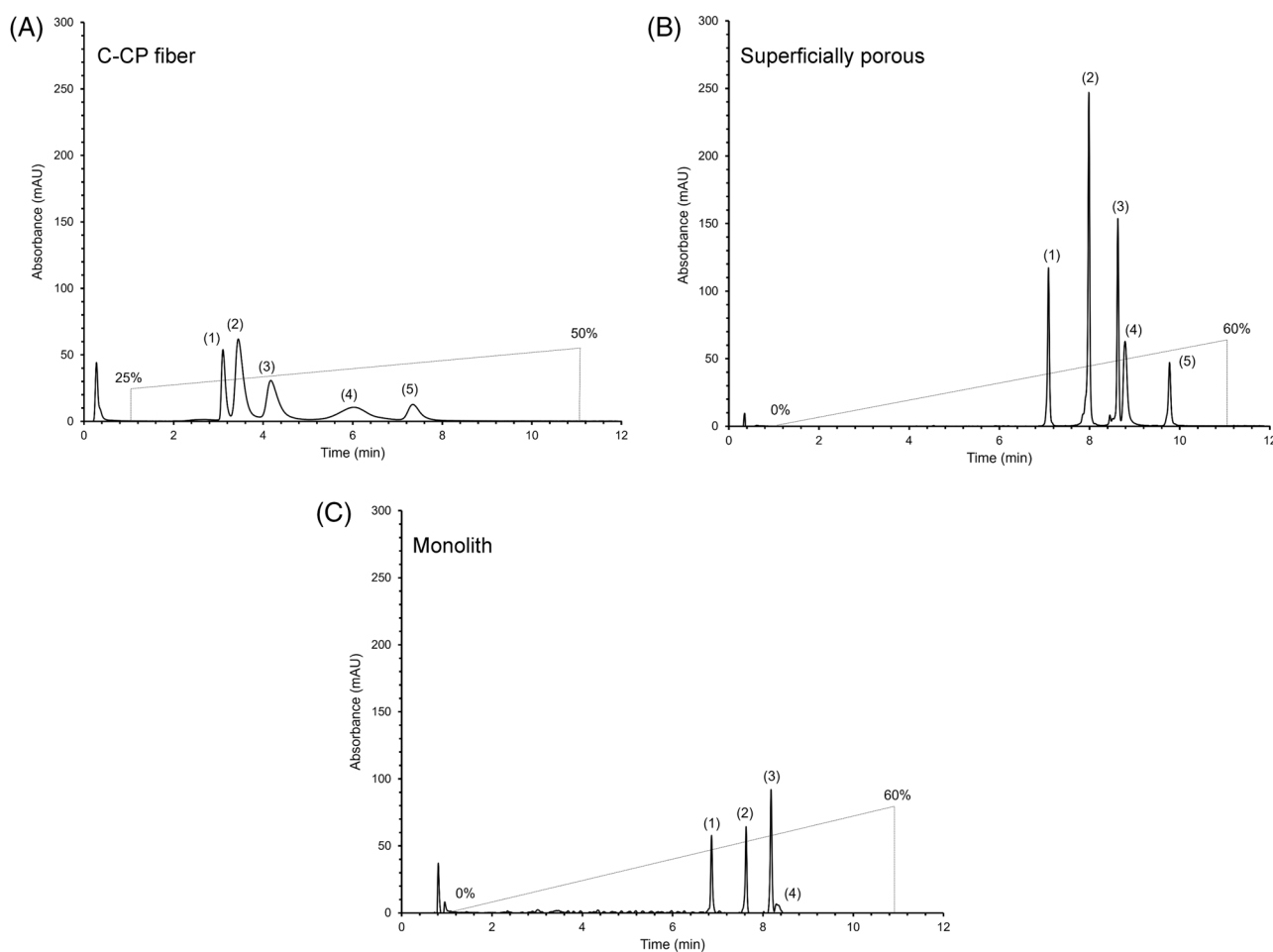


FIGURE 4 Separation of a five-protein ((1) ribonuclease A, (2) cytochrome c, (3) lysozyme, (4) transferrin, (5) α -chymotrypsinogen mixture under optimized conditions. (A) Polypropylene (PPY) C-CP fiber column: gradient 25–50% B (ACN containing 0.1% TFA) in 10 min, flow rate 0.6 ml/min. (B) Superficially porous column: gradient 0%–60% B (ACN containing 0.1% TFA) in 10 min, flow rate 0.8 ml/min. (C) Monolithic column: gradient 0%–60% B (ACN containing 0.1% TFA) in 10 min, flow rate 2.00 ml/min. Each column was regenerated for five min following each run

and the α -chym is not observed in the test gradient window. The following paragraphs provide more qualitative and quantitative comparisons among the column separation characteristics, with the chromatographic figures of merit presented in Table 5.

The first point of comparison between the various phases involves the enthalpic aspects of the respective phases. In terms of raw hydrophobicity, it would be expected that the polypropylene fibers would be the most retentive versus the C18-modified superficially porous and

TABLE 5 Chromatographic characteristics of merit for polypropylene (PPY), superficially porous, and monolithic columns for a five-protein separation ($n=3$) under conditions of Table 4

Column	Protein	% B to desorb protein	Peak half-width ($W_{0.5}$ min)	Resolution (R_s)	Peak area (mAU*min)
PPY	Ribonuclease A	32.3%	0.105	1.17	8.19
	Cytochrome C	33.2%	0.266	1.47	13.1
	Lysozyme	34.9%	0.298	2.24	9.75
	Transferrin	39.4%	0.704	1.57	7.61
	α -Chymotrypsinogen	42.8%	0.291	17.4	4.10
Superficially porous	Ribonuclease A	42.5%	0.0830	6.42	6.35
	Cytochrome C	47.9%	0.0393	6.76	13.6
	Lysozyme	51.8%	0.0410	1.41	7.06
	Transferrin	52.7%	0.0890	8.10	5.51
	α -Chymotrypsinogen	58.7%	0.055	21.8	8.4
Monolithic	Ribonuclease A	41.2%	0.040	11.7	2.38
	Cytochrome C	45.8%	0.037	8.33	3.34
	Lysozyme	49.1%	0.042	7.34	4.14
	Transferrin	49.8%	0.148	4.65	0.605
	α -Chymotrypsinogen	N/A	N/A	N/A	N/A

the C8-modified monolith phases. As seen in Table 5, the %B elution values for each of the proteins tell a different story. It is certainly true that the C18 phase is slightly more retentive than the C8 ligand, as might be expected; approximately 2% B for each of the respective proteins. On the other hand, the proteins elute at appreciably lower (>10% B) solvent strengths from the fiber phase than in the alkyl-ligated phases, as seen in previous comparisons. There may be a few reasons for this relationship, which deserve greater experimental effort in the future. First, as found in previous protein separations on the fibers, it may be that the high shear rates result in lesser amounts of protein relaxation to the stationary phase surface, that is, lesser amounts of adsorption. Second, there may be a level of entanglement of the proteins among the ligand strands on the modified phases, a well-known phenomenon in small molecule separations [70]. Beyond the dominant hydrophobic interactions, there may be additional modes of interaction of the proteins with the two silica-based phases, including with surface silanol species. In general, while not necessarily consequential in the separation quality, the elution of proteins at lower percentages of ACN in the case of the fiber phase may have the positive effect of lesser tendencies of protein denaturation.

In virtually all cases of protein gradient elution, there exists a trade-off between the two components (numerator and denominator) of the resolution equation (Equation (4))

$$R_s = 2(t_{R2} - t_{R1}) / w_1 + w_2 \quad (4)$$

as low gradient slopes increase the temporal displacement of bands but also add to their breadth. These aspects are born out in comparing the eluting peak half-widths and the resulting resolution across the respective column types. As would be expected based on the similarity in the gradient conditions, the two commercial columns yield very comparable peak widths and resulting resolution values. Indeed, the resolution realized across the entire suite on the superficially porous phase is superior to what is achieved on the fiber columns. Here, the practical ramifications of the higher plate heights and shallower gradient of the fiber column lead to peak widths much larger than in the commercial columns. While the resolution of the superficially porous column is clearly superior across the entire suite, it must be noted that there are appreciable perturbations in the baselines of the respective peak profiles. It is not clear what the sources of these satellite peaks may be, but they are not present in other phases. There is appreciable background “noise” in the chromatogram produced by the monolithic column.

One other quantitative measure which can be derived from the representative chromatograms of Figure 4 is the respective recoveries among the three column types. As noted above, it would be entirely expected that narrow, high peak height value responses would be expected for the steeper gradient rates. In this regard, as the same test solution and injection volumes are employed, the integrated absorbance peak areas, and not the peak height values, are of relevance. As seen in Table 4, the solute recoveries of the fiber and superficially porous phases are very simi-

TABLE 6 Repeatability of peak characteristics for lysozyme and bovine serum albumin (BSA) injections ($n = 5$) onto the polypropylene (PPY) C-CP fiber, superficially porous, and monolithic columns. All data is reported as %RSD

Column type	Protein	Retention time (%RSD)	Peak width (%RSD)	Peak height (%RSD)	Peak area (%RSD)
PPY	Lysozyme	0.21	2.5	3.1	2.6
	BSA	1.9	5.1	9.8	10.9
Poroshell	Lysozyme	3.9	29.1	33.1	11.1
	BSA	1.1	11.3	11.7	17.7
Monolithic	Lysozyme	0.020	1.5	7.2	6.5
	BSA	0.092	8.5	7.5	4.3

lar, with those of the monolithic column being appreciably lower (>4X) in the case of the first three eluting proteins, with the recovery of the trans being very much lower and the α -chym A not being observed at all. The potential that solutes might be lost from the chromatograms as they co-elute with other solutes was ruled out by single component injections. It may be that the latter protein is not eluted within the gradient window (up to 60% B). Based on the comparison of eluting solvent strengths for the superficially porous phase, this does not seem reasonable. The fact that the recovery for the trans is also very poor (while still observed) suggests that these proteins are irreversibly bound by some sort of non-ideal surface interactions.

Chromatographic repeatability, without sacrificing performance or resolution, is essential when comparing stationary phases. Inconsistencies across columns, and more importantly for singular columns, may be caused by both physical and surface chemistry instability. Both can affect experimental reproducibility, altering retention times, separation efficiency, peak quality, and recoveries. The variability in retention times, peak widths, peak heights, and peak areas were evaluated for all three of the columns under the optimized conditions. Lysozyme and BSA, which are common protein test species, were used as the protein markers to ascertain whether the molecular weight of the proteins might affect the reproducibility among the columns. Each protein separation was performed 5 times, and the results were tabulated amongst the three columns in Table 6. Across the assembled metrics, there are some very definite differences among the column types as well as for the different proteins. Most striking is the much poorer reproducibility realized for the superficially porous column versus the fiber or monolithic columns. Perhaps surprising, the imprecision is far worse for the lower molecular weight lyso versus BSA. At this point, there are no real hypotheses as to why the repeatability of that column is so much diminished. On the other hand, the experimental repeatability for the fiber and monolithic columns was quite comparable, except for the case of retention time where the monolith was far superior. The measurement precision was fairly equivalent for

the two proteins on the monolithic column, but in the case of the fiber column lyso showed somewhat better performance versus BSA. In general, though, the in-house prepared fiber columns show a high level of measurement stability.

3.4 | Comparison of protein dynamic binding capacity across column types

While there are certainly column formats that are specifically designed for use in preparative-scale protein separations [71], which are very different in structure and operational goals than the 'analytical' columns employed here, it is still instructive to assess protein loading to understand the dynamics and thermodynamics of analytical column phases. The most straightforward, albeit less quantitative, means of assessing dynamic binding capacities involves a simple breakthrough analysis. Basically, a known concentration of protein solution is fed through the column with the absorbance measured post-column to assess the point of column saturation, that is, breakthrough, where the absorbance reaches a steady plateau reflecting the solution phase protein concentration. There are multiple ways to quantitatively assess the amount of protein adsorbed to the column, chosen here is assigning the binding capacity as the volume of solution yielding an absorbance of one-half of the maximum value. As such, the mass adsorbed is the product of the solute concentration and the time to reach the target absorbance. Simple use of breakthrough curves can provide insights into the kinetics of protein adsorption and the accessible surface area that is provided by the stationary/support phase. The shape of the breakthrough curve is a reflection of the adsorption kinetics of a stationary phase. Theoretically, sharper slopes reflect faster adsorption kinetics and longer breakthrough times indicating that more analyte is retained on the column stationary phase. Depicted in Figures 5A,B are representative breakthrough curves for lyso and BSA, respectively, at concentrations of 0.1 mg/ml at a moderate flow rate of 0.5 ml/min for each column.

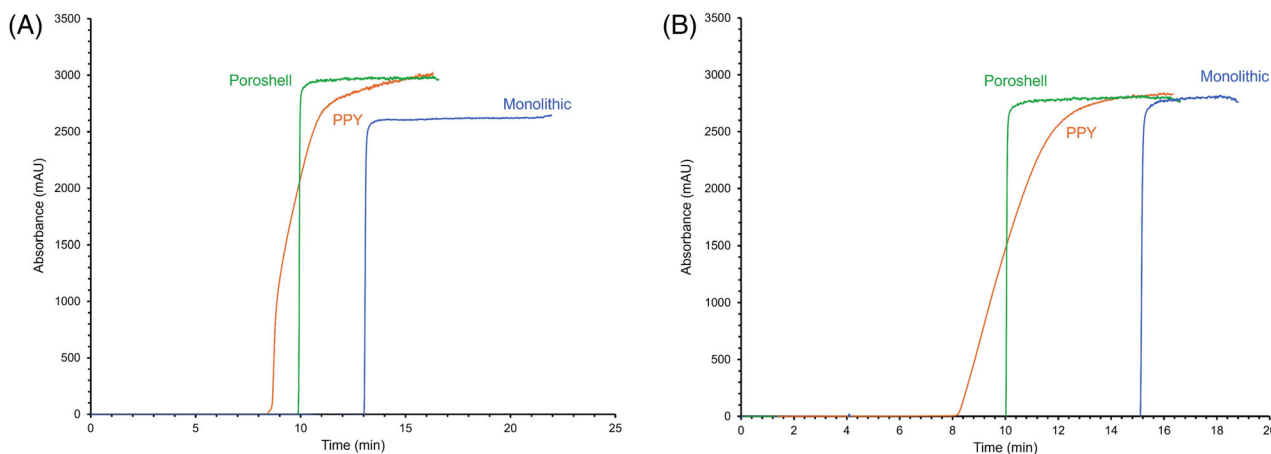


FIGURE 5 Breakthrough curves for the polypropylene (PPY) C-CP fiber column, superficially porous column, and monolithic columns. (A) lysozyme and (B) bovine serum albumin

TABLE 7 Column parameters including length, inner diameter, total column volume, stationary phase bed volume, and the binding capacities for lysozyme and BSA on each column are shown

	Column length (cm)	Column ID (cm)	Total column volume (V_T) (ml)	Packed bed volume (ml)	Lysozyme binding capacity		BSA binding capacity	
					(mg)	(mg/ml)	(mg)	(mg/ml)
PPY	30	0.078	0.137	0.0499	0.458	9.18	0.487	9.76
Superficially porous	5	0.30	0.353	0.128	0.497	3.88	0.503	3.93
Monolithic	10	0.46	1.66	0.602	0.654	1.09	0.758	1.26

The breakthrough curves of Figure 5 illustrate pronounced differences between the fiber format and the commercial columns. First, the longer loading times for the commercial phases reflect higher absolute amounts of bound protein. Second, while saturation appears as a virtual step-function on the superficially porous and monolithic phases, there is a more diffuse response at breakthrough for the fibers. The shape of the fronts on the fiber phase reflects a kinetically-slow adsorption process versus the solute delivery rate (velocity), particularly as the surfaces reach saturation. This response reflects a slow ‘filling’ of available surface area. Here, it must be pointed out that the mobile phase linear velocity, in this case, is ~ 40 mm/s versus ~ 2 mm/s for the other two phases, thus amplifying any mass transport limitations. Indeed, previous studies have shown far more ‘vertical’ breakthrough curves for the fiber phases operated at lower linear velocities. Table 7 presents the physical dimensions of the respective column platforms and the equivalent stationary phase bed volumes, along with the calculated absolute protein masses as well as the capacities per unit of column volume. As can be gleaned from the respective breakthrough times, the capacities for the fiber and superficially porous columns are nearly equivalent, with the monolith accepting $\sim 20\%$ – 50% higher amounts. Another difference lies in the fact that those two phases have very

similar capacities for both proteins, while the monolith loads appreciably more BSA than lyso. Most telling in the loading characteristics is the great disparity in the bed volume-based dynamic binding capacities, averaging ~ 9.5 mg/ml for the C-CP fiber column, ~ 3.9 mg/ml for the superficially porous phase, and 1.2 mg/ml for the monolith. This relationship is particularly interesting given the fact that the fiber phase has specific surface areas on the order of $1 \text{ m}^2 \text{ g}^{-1}$, whereas the other phases provide values of 10–100X more. Thus, the C-CP fiber provides far more efficient access to the useable surface area than the more porous, commercial phases.

4 | CONCLUDING REMARKS

The performance of the PPY C-CP fiber column toward RP separations of a diverse suite of proteins was evaluated by a series of experiments that included the evaluation of the resolution, peak height ($<10\%$ RSD), peak width ($<5\%$ RSD), and peak area ($<11\%$ RSD) characteristics during the RP isolation of a 5-protein suite. Optimization studies for the RP separation of the PPY fiber phases determined a shallow gradient elution window (25%–50% B) over 10 min at higher linear flow velocities (46.4 mm/s) and lower back pressures (~ 4 MPa) yielded overall chromatographic

quality that was competitive with the commercial 'protein' columns. When quantitatively comparing protein separations across the three stationary phases, the monolithic column exhibited superior plate height figures of merit, while the superficially porous column yielded higher resolution across the protein suite; however, perturbations across the baseline were present and poorer reproducibility was exhibited in comparison to the other columns. The fiber and superficially porous phases provided comparably high protein recoveries, while monolith phases produced somewhat lower recoveries (based on eluate peak areas) for the first three eluting proteins, with the trans peak being appreciably lower, and α -chym A not being recovered at all. In contrast to the alkyl-modified phases, the fiber columns required far lower solvent strengths (%B) to elute the proteins. While producing non-ideal breakthrough characteristics, the fiber columns operating at much higher linear velocities yield per-bed-volume binding capacities far greater than the commercial phases. The benefits recognized here, combined with affordability (<\$5), ease of construction (<5 min), and customizability of the fiber phases, make the PPY fiber phase an attractive alternative for chromatographic protein separations. A direct comparison with polymeric monoliths is certainly in order for the future. Additionally, future works will employ the trilobal C-CP fiber shape in new application areas including the isolation/purification of extracellular vesicles [72], virus particles [73], and other nanobodies.

ACKNOWLEDGMENTS

This project was supported in part by the National Science Foundation grant CHE-2107882.


CONFLICT OF INTEREST

The authors have no financial conflict of interest to report.

DATA AVAILABILITY STATEMENT

The data that support the findings of this study are available from the corresponding author upon reasonable request.

ORCID

R. Kenneth Marcus  <https://orcid.org/0000-0003-4276-5805>

REFERENCES

1. Neue UD. HPLC columns: Theory, technology, and practice. New York: Wiley-VCH; 1997.
2. Kirkland JJ. Development of some stationary phases for reversed-phase HPLC. *J Chromatogr A*. 2004;1060:9–21.
3. Ali I, Aboul-Enein HY, Singh P, Singh R, Sharma B. Separation of biological proteins by liquid chromatography. *Saudi Pharm J*. 2010;18:59–73.
4. Cunico RL, Gooding KM, Wehr T. Basic HPLC and CE of biomolecules. Richmond, CA: Bay Bioanalytical Laboratory; 1998.
5. Aguilar M-I, Hearn MT. High-resolution reversed-phase high-performance liquid chromatography of peptides and proteins. *Methods Enzymol*. 1996;270:3–26.
6. Fekete S, Veuthey J-L, Guillaume D. New trends in reversed-phase liquid chromatographic separations of therapeutic peptides and proteins: theory and applications. *J Pharm Biomed Anal*. 2012;69:9–27.
7. Jungbauer A. Chromatographic media for bioseparation. *J Chromatogr A*. 2005;1065:3–12.
8. Kastner M. Protein liquid chromatography. Amsterdam: Elsevier Science; 1999.
9. Mant CT, Hodges RS. High-performance liquid chromatography of peptides and proteins: separation, analysis, and conformation. Boca Raton, FL: CRC Press; 1991.
10. Hanson M, Unger KK, Mant CT, Hodges RS. Optimization strategies in ultrafast reversed-phase chromatography of proteins. *Trac Trends Anal Chem*. 1996;15:102–10.
11. Chen Y, Mehok A, Mant C, Hodges R. Optimum concentration of trifluoroacetic acid for reversed-phase liquid chromatography of peptides revisited. *J Chromatogr A*. 2004;1043:9–18.
12. Guo D, Mant CT, Hodges RS. Effects of ion-pairing reagents on the prediction of peptide retention in reversed-phase high-resolution liquid chromatography. *J Chromatogr A*. 1987;386:205–22.
13. Glajch JL, Kirkland JJ, Köhler J. Effect of column degradation on the reversed-phase high-performance liquid chromatographic separation of peptides and proteins. *J Chromatogr A*. 1987;384:81–90.
14. Wang QC, Svec F, Frechet JMJ. Macroporous polymeric stationary-phase rod as continuous separation medium for reversed-phase chromatography. *Anal Chem*. 1993;65:2243–8.
15. Tanaka N, Araki M. Polymer-based packing materials for reversed-phase liquid-chromatography. *Adv Chromatogr*. 1989;30:81–122.
16. Fulton SP, Afeyan NB, Gordon NF, Regnier FE. Very High-Speed Separation of Proteins with a 20-Mu-M Reversed-Phase Sorbent. *J Chromatogr*. 1991;547:452–6.
17. Bohrer D, dos Santos MV, Ramirez AG, do Nascimento PC, de Carvalho LM. Performance of polymeric materials for solid phase extraction prior to chromatographic analysis. *J Chromatogr B*. 2009;877:277–84.
18. Marcus RK. Use of polymer fiber stationary phases for liquid chromatography separations: part I - physical and chemical rationale. *J Sep Sci*. 2008;31:1923–35.
19. Giddings JC. Dynamics of chromatography. New York: Marcel Dekker; 1965.
20. Giddings JC. Unified separation science. New York: John Wiley & Sons; 1991.
21. Horvath CG, Preiss BA, Lipsky SR. Fast liquid chromatography. Investigation of operating parameters and the separation of nucleotides on pellicular ion exchangers. *Anal Chem*. 1967;39:1422–8.
22. Horvath C, Lipsky SR. Column design in high-pressure liquid chromatography. *J Chromatogr Sci*. 1969;7:109–16.
23. Kaczmarek K, Guiochon G. Modeling of the mass-transfer kinetics in chromatographic columns packed with shell and pellicular particles. *Anal Chem*. 2007;79:4648–56.

24. Gritti F, Guiochon G. Mass transfer mechanism in liquid chromatography columns packed with shell particles: would there be an optimum shell structure? *J Chromatogr A*. 2010;1217:8167–80.
25. Cabrera K, Lubda D, Eggenweiler H-M, Minakuchi H, Nakanishi K. A new monolithic-type HPLC column for fast separations. *J High Resol Chromatogr*. 2000;23:93–9.
26. Fekete S, Fekete J. Fast gradient screening of pharmaceuticals with 5cm long, narrow bore reversed-phase columns packed with sub-3 μ m core-shell and sub-2 μ m totally porous particles. *Talanta* 2011;84:416–23.
27. Kirkland JJ. Superficially porous silica microspheres for the fast high-performance liquid chromatography of macromolecules. *Anal Chem*. 1992;64:1239–45.
28. Wang X, Barber WE, Carr PW. A practical approach to maximizing peak capacity by using long columns packed with pellicular stationary phases for proteomic research. *J Chromatogr A*. 2006;1107:139–51.
29. DeStefano JJ, Langlois TJ, Kirkland JJ. Characteristics of superficially-porous silica particles for fast HPLC: some performance comparisons with sub-2- μ m particles. *J Chromatogr Sci*. 2008;46:254–60.
30. Fallas MM, Buckenmaier SMC, McCalley DV. A comparison of overload behaviour for some sub 2 μ m totally porous and sub 3 μ m shell particle columns with ionised solutes. *J Chromatogr A*. 2012;1235:49–59.
31. Naeem HA, Sapirstein HD. Ultra-fast separation of wheat glutenin subunits by reversed-phase HPLC using a superficially porous silica-based column. *J Cereal Sci*. 2007;46:157–68.
32. Kirkland JJ, Truszkowski FA, Dilks CH, Engel GS. Superficially porous silica microspheres for fast high-performance liquid chromatography of macromolecules. *J Chromatogr A*. 2000;890:3–13.
33. Tanaka N, Kobayashi H, Nakanishi K, Minakuchi H, Ishizuka N. Monolithic LC columns. *Anal Chem*. 2001;73:420A–9A.
34. Svec F, Fréchet JM. New designs of macroporous polymers and supports: from separation to biocatalysis. *Science* 1996;273:205–11.
35. Guiochon G. Monolithic columns in high-performance liquid chromatography. *J Chromatogr A*. 2007;1168:101–68.
36. Li Y, Lee ML. Biocompatible polymeric monoliths for protein and peptide separations. *J Sep Sci*. 2009;32:3369–78.
37. Jungbauer A, Hahn R. Polymethacrylate monoliths for preparative and industrial separation of biomolecular assemblies. *J Chromatogr A*. 2008;1184:62–79.
38. Poddar S, Sharmeen S, Hage DS. Affinity monolith chromatography: a review of general principles and recent developments. *Electrophoresis* 2021;42:2577–98.
39. Brice RW, Zhang X, Colón LA. Fused-core, sub-2 μ m packings, and monolithic HPLC columns: a comparative evaluation. *J Sep Sci*. 2009;32:2723–2731.
40. Czok M, Guiochon G. Aligned fiber columns for size-exclusion chromatography. *J Chromatogr A*. 1990;506:303–17.
41. Hamaker K, Liu JY, Ladisch CM, Ladisch MR. Transport properties of rolled, continuous stationary phase columns. *Biotechnol Prog*. 1998;14:21–30.
42. Marcus RK. Use of polymer fiber stationary phases for liquid chromatography separations: part II - applications. *J Sep Sci*. 2009;32:695–705.
43. Chen LQ, Zhang W, Zhen Z. Study of ion chromatography with ion-exchange fibers as the stationary phase. *J Chromatogr A*. 1996;740:195–9.
44. Bosma JC, Wesselingh JA. Partitioning and diffusion of large molecules in fibrous structures. *J Chromatogr B*. 2000;743:169–80.
45. Li CH, Ladisch CM, Yang YQ, Hendrickson R, Keim C, Mosier N, Ladisch MR. Optimal packing characteristics of rolled, continuous stationary-phase columns. *Biotechnol Prog*. 2002;18:309–16.
46. Ding HB, Yang MC, Schisla D, Cussler EL. Hollow-fiber liquid-chromatography. *AIChE J*. 1989;35:814–20.
47. Kiso Y, Takayama K, Jinno K. Cellulose-acetate as stationary phase in microcolumn LC. *HRC J High Res Chromatogr*. 1989;12:169–73.
48. Nelson DM, Marcus RK. Characterization of capillary-channeled polymer fiber stationary phases for high-performance liquid chromatography protein separations: comparative analysis with a packed-bed column. *Anal Chem*. 2006;78:8462–71.
49. Nelson DM, Marcus RK. Potential for ultrafast protein separations with capillary-channeled polymer (C-CP) fiber columns. *Protein Peptide Lett*. 2006;13:95–9.
50. Randunu KM, Marcus RK. Microbore polypropylene capillary-channeled polymer (C-CP) fiber columns for rapid reversed-phase HPLC of proteins. *Anal Bioanal Chem*. 2012;404:721–9.
51. Stanelle RD, Marcus RK. Nylon-6 capillary-channeled polymer (C-CP) fibers as a hydrophobic interaction chromatography stationary phase for the separation of proteins. *Anal Bioanal Chem*. 2009;393:273–81.
52. Jiang L, Marcus RK. Comparison of analytical protein separation characteristics for three amine-based capillary-channeled polymer (C-CP) stationary phases. *Anal Bioanal Chem*. 2016;408:1373–83.
53. Wang L, Marcus RK. Evaluation of protein separations based on hydrophobic interaction chromatography using polyethylene terephthalate capillary-channeled polymer (C-CP) fiber phases. *J Chromatogr A*. 2019;1585:161–71.
54. Jiang L, Marcus RK. Microwave-assisted, grafting polymerization preparation of strong cation exchange nylon 6 capillary-channeled polymer fibers and their chromatographic properties. *Anal Chim Acta*. 2017;977:52–64.
55. Jiang L, Marcus RK. Microwave-assisted, grafting polymerization modification of Nylon 6 capillary-channeled polymer fibers for enhanced weak cation exchange protein separations. *Anal Chim Acta*. 2017;954:129–39.
56. Jiang L, Marcus RK. Biotin functionalized poly(ethylene terephthalate) capillary-channeled polymer fibers as HPLC stationary phase for affinity chromatography. *Anal Bioanal Chem*. 2015;407:939–51.
57. Schadock-Hewitt AJ, Marcus RK. Initial evaluation of protein A modified capillary-channeled polymer fibers for the capture and recovery of immunoglobulin G. *J Sep Sci*. 2014;37:495–504.
58. Trang HK, Jiang L, Marcus RK. Microwave-assisted grafting polymerization of capillary-channeled polymer (C-CP) nylon 6 fibers for immobilized metal-ion affinity chromatography (IMAC) protein separations. *J Chromatogr B*. 2019;1110:144–54.
59. Marcus RK, Davis WC, Knippel BC, LaMotte L, Hill TA, Perahia D, Jenkins JD. Capillary-channeled polymer fibers as stationary

- phases in liquid chromatography separations. *J Chromatogr A*. 2003;986:17–31.
60. Randunu KM, Dimartino S, Marcus RK. Dynamic evaluation of polypropylene capillary-channeled fibers as a stationary phase in high-performance liquid chromatography. *J Sep Sci*. 2012;35:3270–80.
61. Wang Z, Marcus RK. Determination of pore size distributions in capillary-channeled polymer fiber stationary phases by inverse size-exclusion chromatography and implications for fast protein separations. *J Chromatogr A*. 2014;1351:82–9.
62. Stanelle RD, Sander LC, Marcus RK. Hydrodynamic flow in capillary-channel fiber columns for liquid chromatography. *J Chromatogr A*. 2005;1100:68–75.
63. Wang L, Stevens KA, Haupt-Renaud P, Marcus RK. Dynamic evaluation of a trilobal capillary-channeled polymer fiber shape for reversed-phase protein separations and comparison to the eight-channeled form. *J Sep Sci*. 2018;41:1063–73.
64. Leveque MA. The Laws of Convective Heat Transfer. *Ann Min*. 1928;13:284.
65. Youmans KB, Wang L, Marcus RK. Application of trilobal capillary-channeled polymer (C-CP) fibers for reversed-phase liquid chromatography and ESI-MS for the determination of proteins in different biological matrices. *Anal Methods*. 2019;11:3800–9.
66. Huang S, McClain RT, Marcus RK. Comparison of the separation of proteins of wide-ranging molecular weight via trilobal polypropylene capillary-channeled polymer fiber, commercial superficially porous, and commercial size exclusion columns. *J Sep Sci*. 2022;45:1502–13.
67. Wang L, Marcus RK. Overload effects in reversed-phase protein separations using capillary-channeled polymer fiber columns. *Biotechnol Prog*. 2018;34:1221–33.
68. Bird BR, Stewart WE, Lightfoot EN. *Transport phenomena*. New York: Wiley; 1960.
69. Wang Z, Marcus RK. Roles of interstitial fraction and load conditions on the dynamic binding capacity of proteins on capillary-channeled polymer fiber columns. *Biotechnol Prog*. 2015;31:97–109.
70. Sander LC, Wise SA. Shape selectivity in reversed-phase liquid-chromatography for the separation of planar and nonplanar solutes. *J Chromatogr A*. 1993;656:335–51.
71. Carta G, Jungbauer A. *Protein chromatography: process development and scale-up*. Weinheim: Wiley-VCH; 2010.
72. Bruce TF, Slonecki TJ, Wang L, Huang S, Powell RR, Marcus RK. Exosome isolation and purification via hydrophobic interaction chromatography using a polyester, capillary-channeled polymer fiber phase. *Electrophoresis* 2019;40:571–81.
73. Huang S, Bruce TF, Ding H, Wei Y, Marcus RK. Rapid isolation of lentivirus particles from cell culture media via a hydrophobic interaction chromatography method on a polyester, capillary-channeled polymer fiber stationary phase. *Anal Bioanal Chem*. 2021;413:2985–94.

How to cite this article: Billotto LS, Marcus RK. Comparative analysis of trilobal capillary-channeled polymer fiber columns with superficially porous and monolithic phases toward reversed-phase protein separations. *J Sep Sci*. 2022;45:3811–3826. <https://doi.org/10.1002/jssc.202200410>